Published in final edited form as:
*Proc SPIE*. 2011 February 23; 7901: 790115–. doi:10.1117/12.876514.

# Development of Novel Magnetic Nanoparticles for Hyperthermia Cancer Therapy

**Shiraz M. Cassim**[a], **Andrew J. Giustini**[a,b], **Ian Baker**[a], and **P. Jack Hoopes**[a,b]

[a]Thayer School of Engineering at Dartmouth College, 8000 Cummings Hall, Hanover, NH 03755

[b]Dartmouth Medical School, 1 Rope Ferry Road, Hanover, NH 03755

## Abstract

Advances in magnetic nanoparticle hyperthermia are opening new doors in cancer therapy. As a standalone or adjuvant therapy this new modality has the opportunity significantly advance thermal medicine. Major advantages of using magnetic magnetite ($Fe_3O_4$) nanoparticles are their highly localized power deposition and the fact that the alternating magnetic fields (AMF) used to excite them can penetrate deeply into the body without harmful effect. One limitation, however, which hinders the technology, is the problem of inductive heating of normal tissue by the AMF if the frequency and fields strength are not appropriately matched to the tissue. Restricting AMF amplitude and frequency limits the heat dose which can be selectively applied to cancerous tissue via the magnetic nanoparticle, thus lowering therapeutic effect. In an effort to address this problem, particles with optimized magnetic properties must be developed. Using particles with higher saturation magnetizations and coercivity will enhance hysteresis heating increasing particle power density at milder AMF strengths and frequencies. In this study we used oil in water microemulsions to develop nanoparticles with zero-valent Fe cores and magnetite shells. The superior magnetic properties of zero-valent Fe give these particles the potential for improved SAR over pure magnetite particles. Silane and subsequently dextran have been attached to the particle surface in order to provide a biocompatible surfactant coating. The heating capability of the particles was tested in-vivo using a mouse tumor model. Although we determined that the final stage of synthesis, purification of the dextran coated particles, permits significant corrosion/oxidation of the iron core to hematite, the particles can effectively heat tumor tissue. Improving the purification procedure will allow the generation $Fe/Fe_3O_4$ with superior SAR values.

### Keywords

Magnetic Nanoparticle; Ferrofluid; Hyperthermia; Tumor; Cancer; Synthesis

## 2. Introduction

Despite decades of concentrated research and experimentation the treatment of cancer remains a foremost challenge of modern medicine. Radiotherapy, chemotherapy and surgery have emerged as the standard of care and achieved marked success in treating some, but not all types of tumors. The myriad of manifestations and lack of a complete understanding of their respective etiologies greatly hinder the ability to find universally effective treatments for the disease. The use of hyperthermia has long known to have potential in the field of cancer treatment, however has yet to attain mainstream success.

The effectiveness of any effort to treat cancer is dependent upon achieving sound therapeutic ratio (TR), the ability selectively control cancerous tissue while sparing normal healthy tissue. All successful current treatment modalities have means to produce meaningful TR but are often unable to do so in key circumstances, Surgery relies upon advanced imaging

techniques to define the tumor boundaries and permit the accurate resection of a tumor. TR is determined by tumor location, ability of imaging techniques to differentiate cancerous tissue, the validity of imaging data between capture and surgery, and the margins chosen by the surgeon. However, once the cancer metastasizes and/or moves beyond the imagable border into essential normal tissues, surgery becomes a much less effective option. Radiotherapy utilizes the fact that many cancer lines exhibit inhibited DNA repair and become more sensitive to radiation damage than normal tissues. High TR depends on the cell type of the malignancy, and the ability to deliver a high radiation dose localized to tumor while avoiding critical radiosensitive structures. TR is hindered by radiotolerant lines of cancer, oxygen lean tumor environments, and prior cancer treatments which leave latent damage in normal tissues. Anti-neoplastic chemotherapeutics generally target cells which exhibit rapid division or are unable to effectively eliminate the chemotherapeutic from the intracellular environment. Normal cell toxicity is chemotherapeutics is often sufficiently high to limit TR to non-curative levels.

Hyperthermia has a long history in experimental cancer treatment. The first recorded use of hyperthermia to treat cancer dates back to the $17^{th}$ century BC[i]. In the late $19^{th}$ Century William Coley experimented developed Coley's toxins after observing tumor regression following high fever stemming from erysipelas infection. The $20^{th}$ century saw research into microwave and radiofrequency hyperthermia therapies. Despite this long history of experimentation hyperthermia has yet to become a standard of care. The reasons for this are multi-factorial. Heat dose quantification is challenging because in vivo thermometry can be difficult. Comparing work within the field of hyperthermia is difficult because cell toxicity resulting from hyperthermia exposure increases exponentially and is cell line dependent. Achieving sufficient therapeutic ratio can be challenging with global heating methods because cancer cells are not inherently more sensitive than normal cells[ii]. Instead hyperthermia has relied upon inferior cooling in the tumor micro-environment to achieve TR. The ability to direct thermal dose to cancerous cells but not normal tissue could greatly augment the therapeutic potential of hyperthermia. For this reason, nanoparticle based heating modalities have been investigated recently. Nanoparticle heat sources offer a highly localized means of power delivery and lend the possibility of targeting on the cellular level.

Magnetic nanoparticle hyperthermia (mNPH) in particular has been the subject of much recent research and development. One key advantage and limitation of using magnetic materials as the heat source is the need for an AMF to activate the particles. The AMFs used to energize magnetic nanoparticles are deeply penetrating which allows particle excitement when deep within tissues in hard to treat locations. The AMF however also inductively heats normal tissues via eddy currents, potentially damaging healthy cells. Eddy current heating scales with the second power of field strength, frequency and treatment volume. To prevent normal tissue toxicity, field intensity and frequency must be kept as low as possible. Unfortunately keeping AMF frequency and fields strength low reduces the heating potential of magnetic nanoparticles and their effect on cancerous tissue. The eddy current problem necessitates quality nanoparticles which have magnetic properties that lend high Specific Absorption Rate (SAR), which is defined as power deposition per gram of material at a given AMF field of fixed strength and frequency. The saturation magnetization ($M_{s)}$ and coercivity of a material determine how much energy is released to the particles surrounding during hysteresis heating, maximizing these properties is required to optimize SAR.

Magnetite remains the material of choice for the field because of its established record of safety and good magnetic properties. Research has lead to many different ways to synthesize magnetite particles. The most conventional method is the coprecipitation of 2:1 mixture of $Fe^{3+}$ and $Fe^{2+}$ via the anaerobic addition of a base. Coprecipitation techniques generally provide a wide particle size distribution with particle morphology highly dependent on

reaction conditions such as temperature, ph, salt species present, base addition rate, and stirring speed[iii]. Iron oxide nanoparticles have also been produce using hydrothermal methods. Hydrothermal synthesis routes typically involve aqueous crystallization in high temperature and high vapor pressure and have been shown to produce highly crystalline nanoparticles with high saturation magnetizations[iv,v]. Other common synthesis methods include thermal decomposition of iron precursors[vi], solgel methods[vii]. There also exist nanoreactor methods; a prime example of this is the use of microemulsion, dispersions of immiscible phases stabilized by a surfactant. These methods are adept at producing extremely small particles with tight size distributions. Vidal-Vidal used a water-in-oil microemulsion to produce highly monodisperse small magnetite particles with diameters of 3.5nm ±0.6nm[viii].

Surface engineering of magnetic nanoparticles is an extremely important to their design. Nanoparticle coatings must afford colloidal and chemical stability while remaining biocompatible. Although many molecules can available to stabilize a Ferrofluid, the most common coating materials for nanoparticles designed for in-vivo work are inorganic silicon or gold based coatings or polymeric coatings. For example, Jorden et al. use aminosilane coated magnetite particles in their 2007 clinical trial[ix]. Prominent polymeric coatings are dextran and polyethylene glycol (PEG). Dextran, a glucan polymer, is often praised for its biocompatibility. Also, Dextran adsorption to magnetite surfaces in situ during nanoparticle synthesis is facilitated by hydrogen bonding of hydroxyl groups to the metal oxide[x]. PEG is another favored biocompatible surfactant because give nanoparticles stealthy characteristics which prevent phagocytosis of the particles by macrophages in the liver and spleen[xi].

In this study, Fe nanoparticles with a magnetite shell are synthesized using a water in oil microemulsion procedure developed in our group[xii]. In a similar fashion as Barrea et al.[xiii] these particles are then given a silane coating which is covalently bonded to dextran to form a double layer biocompatible surfactant coating. Fe has superior bulk magnetic properties to magnetite, $M_{sFe}$= 218emu/g vs. $M_{s,magnetite}$= 92emu/g. It is thought that introducing a core of zerovalent Fe will augment SAR by increasing the particles Ms and coercivity. The magnetite shell serves as a passivation layer to help protect the Fe core from oxidation. The particles are characterized and tested in a mouse tumor model

## 3. Methods and Materials

All chemicals used are reagent grade. Octane, Trimethylamine n-oxide dihydrate, $FeCl_3$ and $NaBH_4$ were acquired from Acros. Hexadecyltrimethylammonium bromide (CTAB), tetramethylammonium hydroxide pentahydrate (TMAH), 2-(*N*-morpholino)ethanesulfonic acid (MES), carboxymethyl dextran, 1-butanol, N-Hydroxy-succinimide(NHS), 1-ethyl-3-(3-dimethylaminopropyl) carbodiimide (EDC), Ammonium Acetate, L-ascrobic acid, neocuprine, ferrozine, and 3-aminopropyl-trimethoxysilane (APTMES) are acquired form Sigma-Aldrich. Toluene, Hexanes and methanol are from Fisher Scientific.

Electron Micrographs are acquired using a Technai F20ST Field Emission Gun Transmission Electron Microscope and a XL-30 Environmental Scanning Electron Microscope with a Field Emission Gun, both of the these microscopes are produced by FEI company.

The AMF is created using a Huttinger (Farmington, CT) TIG 10/300 RF Generator which through a Huttinger designed bus circuit is connected to either an in-vivo mouse induction coil designed and built by Fluxtrol Inc (Auburn Hills, Michigan) or an in-vitro coil created by winding copper tubing.

### 3.1 Synthesis of Ctab Coated Fe/$Fe_3o_4$ Nanoparticles Via Water in Oil Microemulsion

Two water-in-oil microemulsion are created one containing $FeCl_3$ aqueous solution, the other with $NaBH_4$ aqueous solution. First, DI water is degassed by boiling and then cooling in a filter flask under flowing Argon with the mechanical agitation provided by a magnetic stir bar. Once the water has reached room temperature, solutions of 0.2M $FeCl_3$ and 0.85M $NaBH_4$ are made of equal volumes in separate vials which are flooded with argon and capped. The oil phase is prepared by combing octane and n-butanol in a 1:1.43 volume ratio, in two filter flasks. The amount of octane used is determined by the desired oil to water volume ratio, in this case 2:1. To these flasks 0.19g of CTAB per ml of octane is added. The $FeCl_3$ solution and $NaBH_4$ solutions are each added to one of the oil containing flasks. Each flask is agitated via magnetic stirring for 45 minutes under flowing argon. The $NaBH_4$ emulsion is quickly and carefully transferred to two 60ml syringes, limiting air exposure as much as possible. The two syringes are loaded into a syringe pump which is used to slowly introduce the $NaBH_4$ emulsion to the $FeCl_3$ emulsion which is still being agitated at high speed in filter flask under flowing argon. Flow rate is such that transfer completes in 10min depending on the volume of emulsion. The emulsion is then left to react while under argon and agitation for an additional 30 min. The product of this reaction is pure Fe nanoparticles coated in CTAB adsorbed from the emulsion. The magnetic stir bar is removed and a strong magnet is used to concentrate the particles to the bottom of the flask. The emulsion supernatant is poured into a waste container for disposal. The particles are then washed with degassed DI water and methanol which has been degassed via sonication under house vacuum. The particles are suspended in methanol and transferred to a pre-weighed bottle, where they are concentrated magnetically while excess methanol is poured off.

### 3.2 Surface Oxidation of Zero-Valent Iron Nanoparticles

The as-synthesized Fe particles are very reactive. In a dry state, if left un-passivated, the particles are pyrophoric and will destroy themselves upon contact with air. The surface of the particles needs to be carefully oxidized to magnetite. Under flowing argon the particles are dried and weighed, 12-14% of the particle mass of trimethylamine n-oxide is measured out. The particles are then suspended in a volume of IPA large enough to effectively disperse them; to this suspension the trimethylamine n-oxide is added under argon. The bottle containing the particles is sealed and the mixture is left to react under sonication for 45min. The particles are then washed with methanol and dried once more under flowing argon in glass bottle. After drying the argon flooded bottle is capped and transferred to vacuum desiccators where it is left to rest for 2 days. After two days, the bottle is cap is then cracked open and the bottle quickly returned to the vacuum desiccator to passivate an additional day.

### 3.3 Ctab Removal

CTAB must be removed because it is not a biocompatible coating. To remove CTAB, tetramethylammonium hydroxide (TMAH) is used as a phase transfer catalyst and surfactant. Deionized water is degassed, as described before, and used to make a 25% w/w solution of tetramethylammonium hydroxide pentahydrate. CTAB coated nanoparticles are dispersed in hexane in a glass bottle and to this the TMAH is solution is added. The bottle is flooded with argon and sealed. A clear division is visible between the water and hexane phases and the nanoparticle currently remain suspended only in the hexane. The bottle is shaken and sonicated until the particles disperse in the water phase and not the hexane. The particles are concentrated with a strong magnet while the water and hexane are decanted. After washing twice with methanol the particles are dried under flowing argon.

### 3.4 Surface Amination with 3-Aminopropyltrimethoxysilane (Aptmes)

The particles are to be coated with an amino silane molecule to allow dextran to be covalently linked to the particle surface. Post CTAB removal, the nanoparticle powder product is placed in a bottle filled with 40m hexane and 6ml APTMES and placed in a bath sonicator with argon flowing through the top of the bottle. The particles will not disperse well in hexane, but will rather cling to the sides and bottom of the bottle. After 10 min of sonication, 200μl of glacial acetic acid is introduced to the mixture. The bottle is capped to ensure an inert atmosphere and left to sonicate for up to 6 days. As the silane molecules associate with the particle surface the particles begin to adopt a more liquid like appearance and begin to collect in pools along the bottom and sides of the glass bottle. A magnet is used to immobilize the particles in the glass while the hexane solution is decanted. The particles are rinsed with hexane twice and then dispersed in methanol and transferred to a flat bottomed boiling flask, where methanol medium is replaced with toluene. The flat bottom boiling flask is attached to a Dean-Stark extraction apparatus, with input for argon, and a reflux condenser. The toluene is boiled for 6 hrs under argon to remove trace water and promote silane condensation on the particle surface. The particles are carefully dried under argon in the boiling flask, then dispersed in methanol, transferred to a bottle, dried under flowing argon, and placed in a vacuum desiccators for storage.

### 3.5 Amide Linkage of Carboxymethyl Dextran to Particle Surface

To complete the biocompatible surfactant coating dextran will be attached to the particle via the amine groups on the magnetite surface. This process could also be used to attach carboxymethyl PEG should that be desired instead. MES buffer is made to a pH of between 4.5 and 5, using degassed deionized water. Aminated nanoparticles are suspended in 30ml of MES buffer in a sonic bath under flowing argon in a glass bottle. A separate 5ml aliquot of MES buffer is combined with 500mg of CM Dextran, EDC, and NHS. This mixture is sonicated for 30 minutes under argon before being added to the nanoparticle suspension. The glass bottle is flooded with argon before being capped. The reaction is carried out in a covered sonic bath for 24hours. During this time the carboxymethyl group is bonded to the silanenanoparticle surface complex via amide linkage. The dextran coated particle suspension is too stable to be purified by magnetic field. Methanol is degassed by sonication under house vacuum and added to the nanoparticle, buffer suspension. This reduces the solubility of the particles allowing them to be purified via centrifuge. The nanoparticle pellet is rinsed with methanol and dried under argon before being transferred to a vacuum desiccator for storage.

### 3.6 Colorimetric Assay to Determine Iron Content of Various Nanoparticle Schemes

There are various methods to quantify the iron content of a given nanoparticle such as ICP-MS, Atomic Absorption Spectophotometry, and a colorimetric ferrozine assay. We have chosen to employ the later because it is quick accurate and affords our lab autonomy. Nanoparticle samples are weighed out in the 10mg range and digested for several hours in trace metal grade hydrochloric acid. A working reagent is created from DI water, 5M Ammonium Acetate, 2M L-ascorbic acid, 13.1mM neocuprine, and 6.5mM ferrozine (3-(2-Pyridyl)-5,6-diphenyl-1,2,4-tiazine-p.p'-disulfonic acid monosodium salt hydrate). Digested samples are diluted to 30mg/ml while the Fe standard is diluted to 30,24,18,12, and 6 mg/ml. Trace metal HCl is diluted in the same fashion as the samples and used as a blank Samples, blanks, and standards are combined in a 96 well plate with the working reagent in a 1:2 ratio leaving sample concentration in the well at 10mg/ml of particle, and standards at 10, 8,6,4,2 and 0 mg/ml of iron. After 30 min incubation a plate reader is used to measure absorbance of all wells and to generate standard curves sample measurements.

### 3.7 Sar Measurement

One fundamental heating metric by which nanoparticles are compared against each other is SAR. It is the fundamental measure of a particle's capability to deliver a therapeutic thermal dose. To assess particle SAR we suspend the particle sample to an Fe concentration of 11mg/ml in deionized water via sonication. The suspension is cooled to room temperature under Ar. A copper tubing solenoid is attached to the 10kW LRC generator circuit bus and is calibrated using an oscilloscope and magnetic probe. The suspended particles are transferred to a 0.5 ml centrifuge tube which is placed in a Styrofoam insulator that sits in the solenoid. A temperature probe is placed in the middle of the suspension, and temperature is recorded at varying fields strengths, over the course of a minute. For each field, strength plain DI water is also heated to record the SAR present due to inductive heating of the water. SAR is calculated from the rate of temperature increase in the nanoparticle suspension, corrected by the heating data for plain water.

### 3.8 Tumor Model and In-Vivo Treatment

Our $Fe/Fe_3O_4$ nanoparticles are assessed for in vivo tumor efficacy using the MTGB, a mouse mammary adenocarcinoma model developed by Clifton et al.,[xiv,xv]. Cells are cultured in 1× Alpha MEM and suspended at a concentration of 10 million cells per ml. C3H mice (Charles River, Wilmington MA) are chosen for this tumor model. 100μl of cells suspension is injected intradermally into the mouse's flank. Tumors are measured along three primary axis daily are allowed to grow. Tumor volume is calculated as an ellipsoid, when a tumor reaches a volume of $150mm^3$ +/- $40mm^3$ the mouse is treated. Dextran coated nanoparticles are suspended in DI water at a concentration of 28mg/ml. The mouse treatment coil is attached to the 10kW generator and calibrated in the same fashion as the SAR coil. The treated mouse is anesthetized with isoflurane, X number of μl is injected into the tumor and the mouse is immediately taken for treatment. A fiber optic temperature probe containing three sensors each 2mm apart is inserted along the long axis of the tumor, such that temperature can be measured at the skin, peritumor, and central tumor. Another fiber optic probe is inserted into the mouse's rectum to monitor rectal body temperature. The mouse is loaded into the treatment coil and the AMF field is activated. The quantification and comparison of therapeutic heating has historically been challenging, due to the exponential relationship between exposure temperature and cell toxicity and the large variation in the uniformity in heat delivery from various heating modalities. Currently, the use of the cumulative equivalent minutes (CEM) algorithm is the most useful and accurate technique to quantify thermal dose. The FISO temperature monitoring system is accurate to 0.1°C and is capable of calculating CEM, in real time. The tumor is heated until a dose of 60 CEM is reached. When needed high field (700Oe) pulsing is used to reach higher inter tumor temperatures. Rectal temperature is monitored and never allowed to rise above 41.5° C. Upon completion of heating to 60 CEM, the field is deactivated and the mouse allowed to recover. Twenty-four hours after treatment, the mouse is sacrificed and the tumor is excised for treatment. On the same mouse a tumor on the opposite flank is exposed to the AMF without particles present as a control. Additionally, a tumor was injected with particles and left for 24hrs before sacrifice and excision; this tumor was not exposed to the AMF with particles present. Tumors are fixed in glutaraldehyde and processed for light and electron microscopy. Two stains are used: Prussian Blue, and H&E, which provide indicators for iron presence and morphologic assessment, respectively.

## 4. Results and Discussion

The microemulsion method is capable of creating highly crystalline nanoparticles with diameters in the 18-22nm range. When coated with CTAB these particles are about 85% Fe and have $M_s$ in the 100 emu/g range, which is improved over magnetite nanoparticles.

Figure 1 is a transmission electron micrograph showing $Fe/Fe_3O_4$ nanoparticles with appropriate diameters. particle diameters indicated. Figure 2 shows the electron diffraction pattern of these particles indicating a high degree of crystallinity. Diffraction rings for BCC Fe and FCC $Fe_3O_4$ are both present.

The silanization process is carried out slowly in organic media to encourage silane monomer adsorption onto the particle surface over silane polymerization which occurs rapidly in aqueous environment. The desired result is a thin but uniform silane layer on the particle surface a condensation reaction on the surface produces water leaving a siloxane bond joining the particle surface to the silane monomer. Boiling this mixture in toluene removes water from the system in order to drive said condensation reaction forward. After this procedure is complete the particles are reduced 72% Fe and display markedly increased water solubility. After attachment of the CM dextran significant oxidation is encountered during purification. Oxidation is evident as red particle slurry appearing at the top of the suspension after centrifugation; this is indicative of the formation of hematite. It is likely that incubation in the acidic MES buffer promotes rapid oxidation once argon protection is removed during purification. Once the particles are removed from the MES buffer further oxidation is not noticed. Since the dextran coating is effective at maintaining a stable nanoparticle suspension under strong magnetic fields the only quick purification method is centrifugation. This however, allows the oxidized particle slurry to mix with the unoxidized Ferrofluid, reducing the overall saturation magnetization. When examined with the VSM it is observed that saturation magnetization falls to 60emu/g. Iron content of the dextran coated particles reveals that only 15% of dry particle stock is composed of Fe. This likely means that a significant amount of free dextran becomes incorporated into the stock. Figure 3 demonstrates two electron micrographs of the same group of particles. The left image is taken with a scanning transmission electron microscope (STEM) sensor attachment which shows the transmitted signal producing contrast where the Iron cores are and to lesser extent where the silane coating is. The right image is taken in scanning electron mode which produces contrast at the coating boundary. By comparing these images we can see that the dextran coating is about 20-30 nm thick.

The SAR of the dextran coated particles at 500 Oe is 60.8 $W/g_{Fe}$. Due to oxidation this SAR is much lower than we have seen in similar $Fe/Fe_3O_4$ which had SAR measurements of at least 170 $W/g_{Fe}$.

Having accounted for the Iron content a proper amount of particle stock was suspended to ensure iron concentration of 28mg/ml for tumor treatment. The particles heated well enough to deliver a tumor dose of CEM 60. Heating data for tumor treatment is shown in figure 4.

Figure 5 shows the intercellular diffusion of $Fe/Fe_3O_4$ nanoparticles, 1hr after the injection of the nanoparticle suspension. Figure 6 demonstrates the effect of the treatment, complete necrosis is shown resulting from the injection of 30μl of $Fe/Fe_3O_4$ nanoparticles suspended at an Fe concentration of 28mg/ml.

## 5. Concluding Remarks

Using microemulsion methods, core/shell composite $Fe/Fe_3O_4$ nanoparticles have been synthesized. These particles combine the superior magnetic properties of iron with the desirable surface chemistry of magnetite. Surface modification with biocompatible aminosilane covalently coupled to carboxymethyl dextran yields a particle which display good colloidal stability. These novel particles have effectively heated an MTGB mouse mammary adenocarcinoma model to deliver a CEM of 60 and a global temperature as high as 46°C. Although effective, this particle complex could be further optimized; by preventing the corrosion that accompanies the dextran coating procedure. Neutralization of the acidic

MES buffer prior to particle purification may prevent this oxidation greatly enhancing particle SAR. These core/shell composite particles would then offer significant improvements over the state of the art.

## References


1. Breasted, JH. The Edwin Smith surgical papyrus. In: L, S., editor. Therapeutic heat and cold. 2nd. Waverly Press; Baltimore: 1930.
2. Roizin-Towle L, Pirro JP. The Response of Human and Rodent Cells to Hyperthermia. International Journal of Radiation Oncology, Biology, Physics. 1991; 23:751.
3. Wu W, He Q, Jiang C. Magnetic Iron Oxide Nanoparticles: Synthesis and Surface Functionalization Strategies. Nanoscale Res Lett. 2008; 3:397–415. [PubMed: 21749733]
4. Wu W, He Q, Jiang C. Magnetic Iron Oxide Nanoparticles: Synthesis and Surface Functionalization Strategies. Nanoscale Res Lett. 2008; 3:397–415. [PubMed: 21749733]
5. Mao B, et al. Synthesis of magnetite octahedrons from iron powders through a mild hydrothermal method. Materials Research Bulletin. 2006; 41:2226–2231.
6. Park J, Lee E, et al. One-nanometer-scale size-controlled synthesis of monodisperse magnetic iron oxide nanoparticles. Angewandte Chemie-International Edition. 2005; 44(19):2872–2877.
7. Wang, Qun, et al. Synthesis of Nanocrystalline Magnetite ($Fe_3O_4$) Films by Self-Reduction Sol-Gel Route. Materials Science Forum. 2003; 423-425:569.
8. Vidal-Vidal J, et al. Synthesis of monodisperse maghemite nanoparticles by the microemulsion method. Colloids and Surfaces A: Physicochem Eng Aspects. 2006; 288:44–51.
9. Mair-Hauf K, et al. Intracranial thermotherapy using magnetic nanoparticles combined with external beam radiotherapy: results of a feasibility study on patients with gioblastoma multiforme. J Neuro-Oncol. 2007; 81:53–60.
10. Bautista MC, Bomati-Miguel O, et al. Surface characterisation of dextran-coated iron oxide nanoparticles prepared by laser pyrolysis and coprecipitation. Journal of Magnetism and Magnetic Materials. 2005; 293(1):20–27.
11. Tiefenauer LX, Tschirky A, Kühne G, Andres RY. In vivo evaluation of Magnetite Nanoparticles for use as a Tumor Contrast Agent in MRI. Magn Reson Imaging. 1996; 14:391. [PubMed: 8782177]
12. Zhang G, et al. Surface engineering of core/shell iron/iron oxide nanoparticles from microemulsions for hyperthermia. Materials Science and Engineering C. 2010; 30:92–97. [PubMed: 21833157]
13. Barrera C, et al. Surface modification of magnetite nanoparticles for biomedical applications. Journal of Magnetism and Magnetic Materials. 2009; 321:1397–1399.
14. Clifton KH, Briggs RC, Stone HB. Quantitative Radiosensitivity Studies of Solid Carcinomas *in vivo*: Methodology and Effect of Anoxia. Journal of the National Cancer Institute. 1966; 36:965–974.
15. Clifton KH, Drapers NR. Survival-curves of Solid Transplantable Tumor Cells Irradiated *in vivo*: A Method of Determination and Statistical Evaluation; Comparison of Cell-survival and 32P-uptake into DNA. International Journal of Radiation Biology. 1963; 7:515–535.

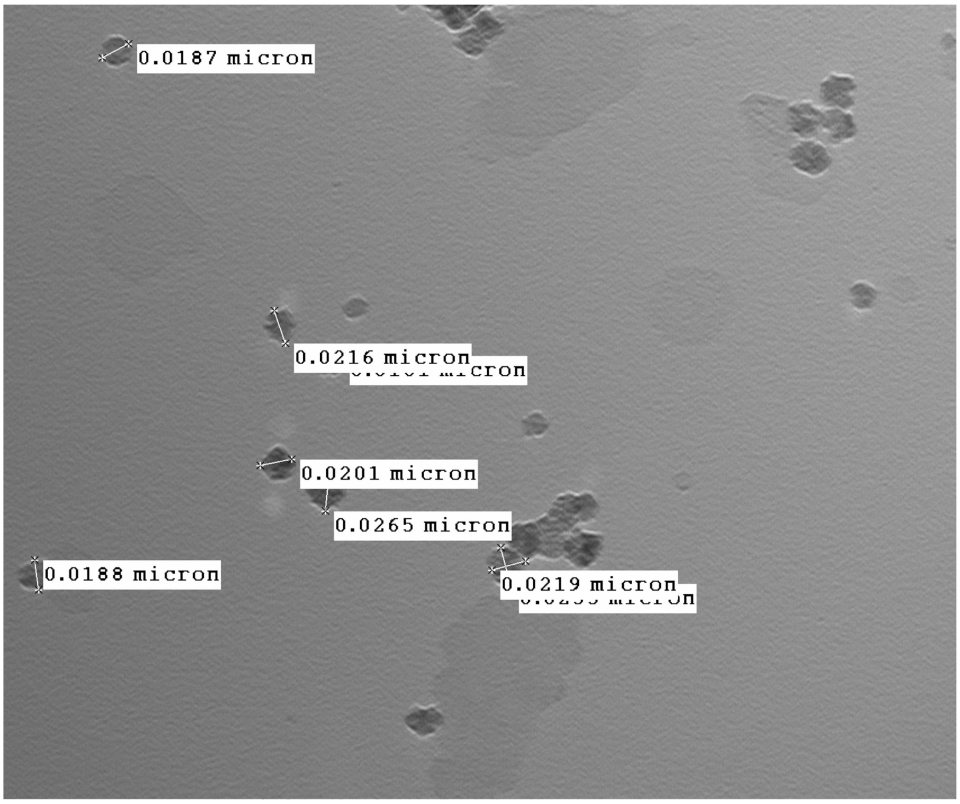


**Figure 1.**
TEM of CTAB Coated Nanoparticles produced with a 2:1 Oil to Water Ratio. Nanoparticles show good crystallinity with cubic grains. Diameters are generally in the 18 to 22nm range.

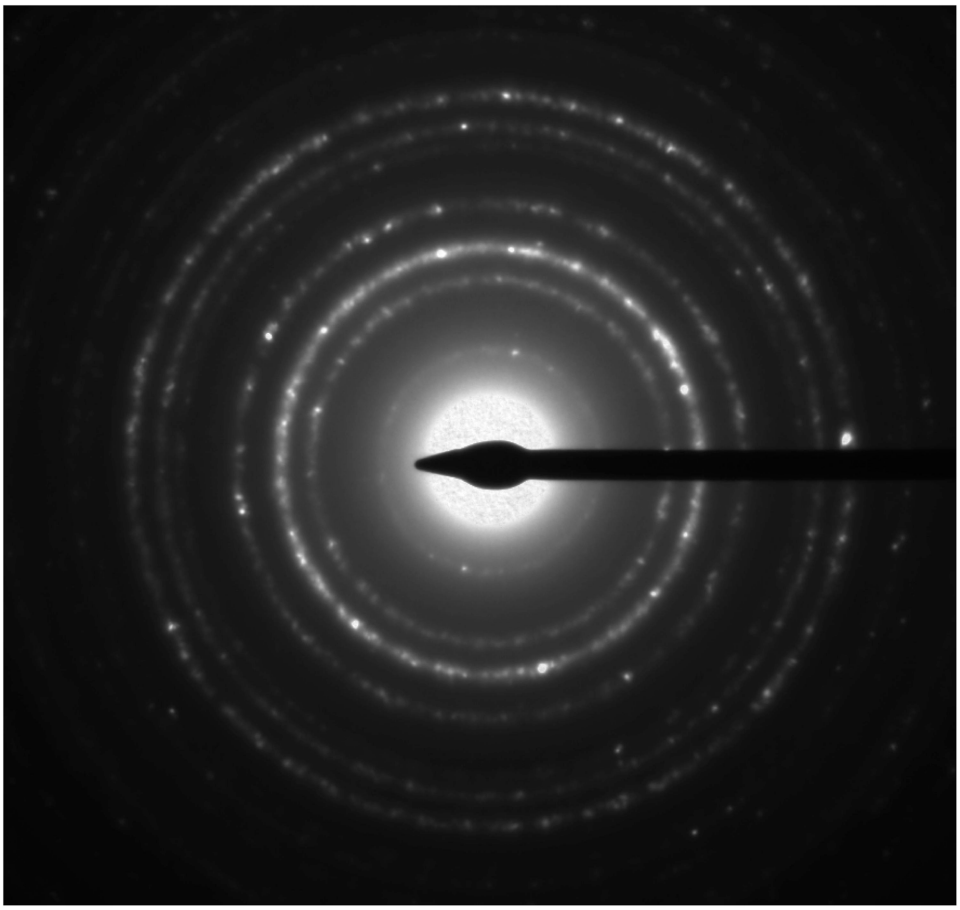

**Figure 2.**
Electron Diffraction Pattern from $Fe/Fe_3O_4$ nanoparticles. Diffraction rings from both the BCC Fe phase and the FCC Magnetite phase are present.

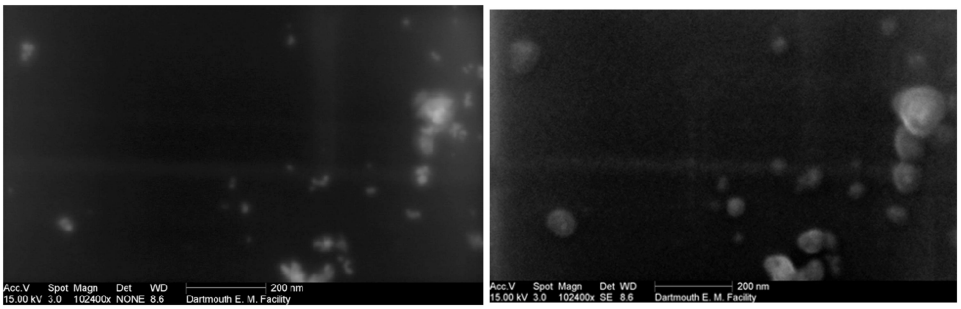


**Figure 3.**

Scanning Electron Micrographs showing signal recorded with STEM attachment (left picture) and standard secondary electron detector (right picture). The STEM signal produces more contrast where the particle cores are located leaving the coating non-visible. The secondary electron signal shows contrast where the coating is. Comparing these two micrographs shows that the dextran coating is approximately 20-30nm thick.

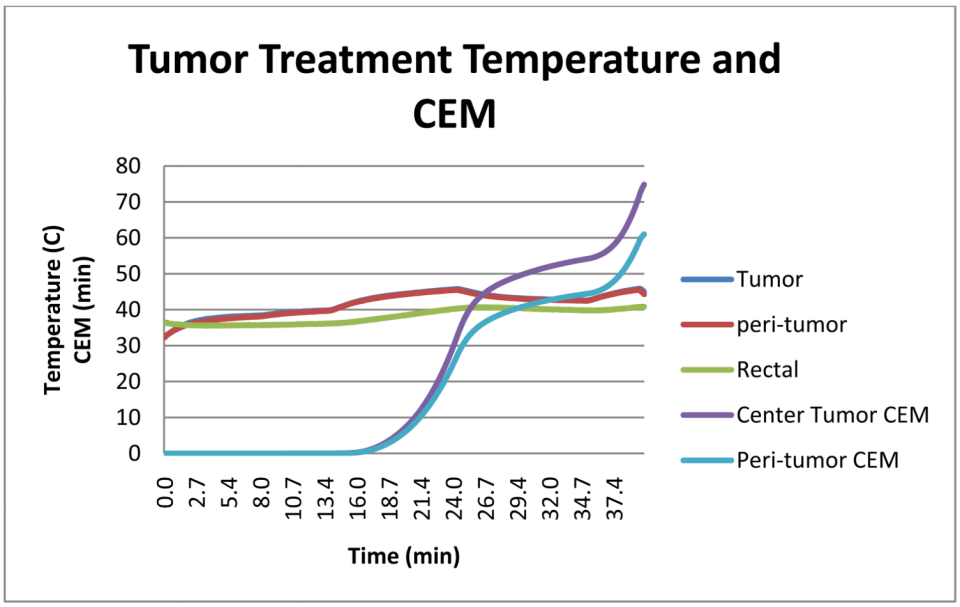


**Figure 4.**
Temperature Monitoring of tumor treatment with dextran coated $Fe/Fe_3O_4$ particles. The peri-tumor received a thermal dose of 60 CEM. The tumor center relieved a dose of about 75 CEM.

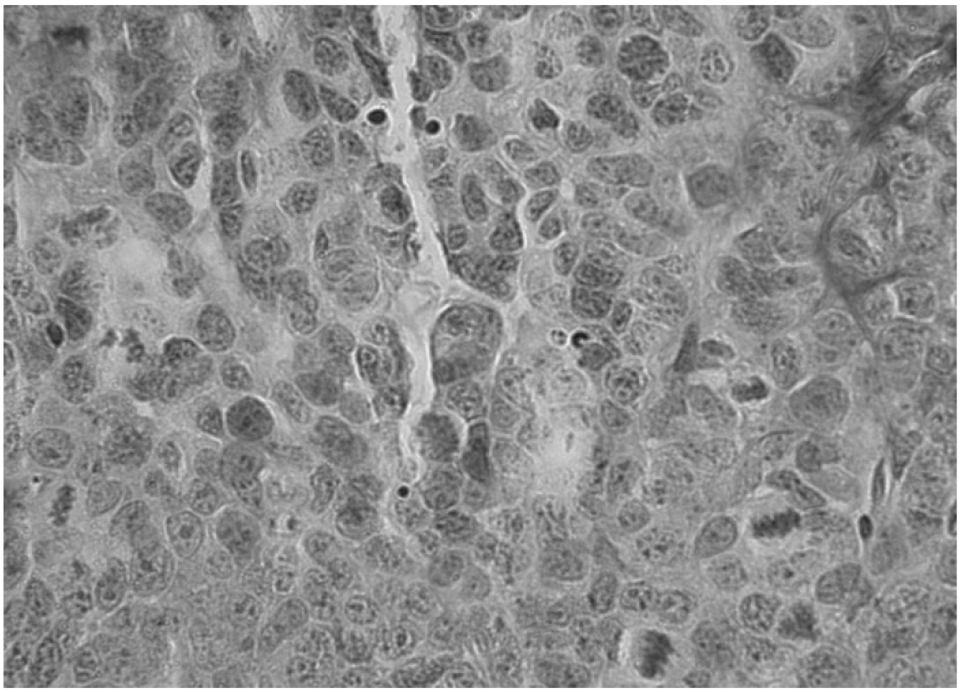

**Figure 5.**
High Magnification photomicrograph of MTGB mouse mammary adenocarcinoma demonstrating $Fe/Fe_3O_4$ nanoparticles situated in the interstitium between tumor cells 1hr post injection. At this time point few nanoparticles have been taken up by the cancer cells, therefore virtually all magnetic nanoparticles remain in the interstitium or on the external plasma membrane. The nanoparticles are most easily seen in the upper right quadrant of the picture.

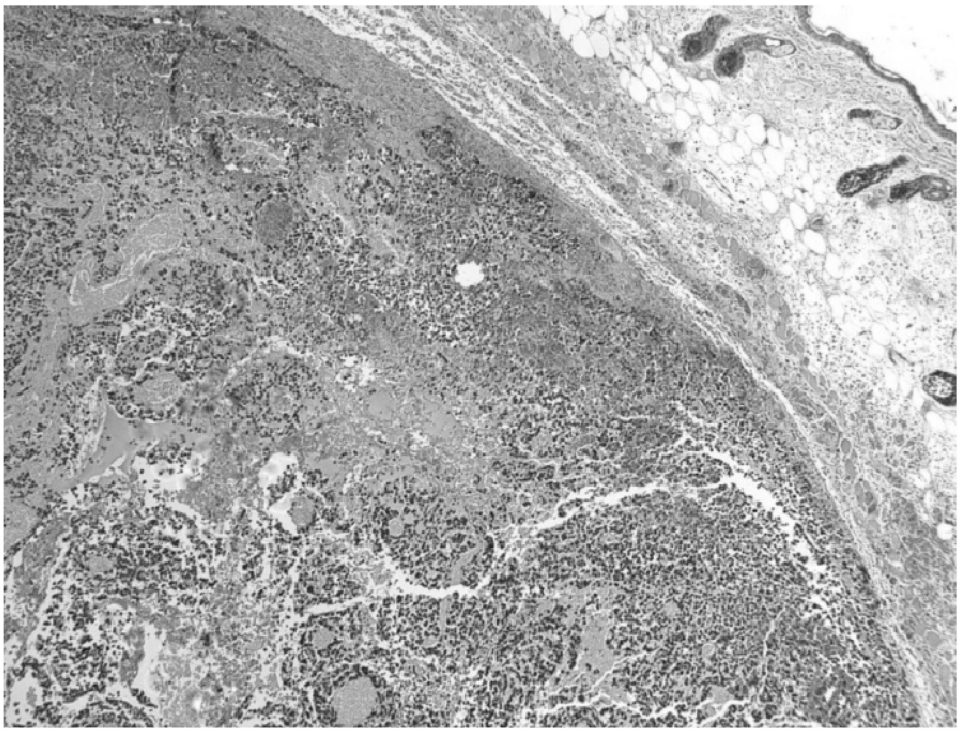

**Figure 6.**

Low magnification photomicrograph demonstrating complete necrosis of an intra-dermally implanted MTGB mouse mammary adenocarcinoma. The treatment effect resulted from the direct injection of 30μl of $Fe/Fe_3O_4$ nanoparticles suspended at Fe concentration of 28mg/ml. $Fe/Fe_3O_4$ particles were activated by 169 kHz AMF to a CEM of 60.